



Türk Fizik Derneği
1950
Turkish Physical Society

e-BOOK of FULL TEXT PROCEEDINGS

**Turkish Physical Society 35th International Physics
Congress (TPS35)**

04-08 September 2019

Bodrum-Muğla / TURKEY

Editors

Baki AKKUŞ

Feyza GÜZELÇİMEN

Barış KINACI

Yeşim YALÇIN

Doğukan BİNGÖL

Çağlar ÇETİNKAYA

Merve SİRKECİ

Erman ÇOKDUYGULULAR

ISBN:978-605-83516-6-0

Contents

01. Applied Physics	1
Producing of CuS Thin Films by Different Coating Methods and Investigation of Optical Properties.....	2
Investigation of Physical Properties and Antibacterial Activity of Ce-Doped Chitosan Nanofibers Obtained by Electrospinning Process.....	10
Assessment of Acoustic Performance of Stratified Composites Prepared from Recycled Paper and Polyurethane Foam.....	17
Nanostructured TiO ₂ Layer Thickness Dependence of the Surface Morphology and Acoustic Impedance.....	23
Generation of Programmable Diffractive Lenses with Multiple or Multi-Optical Axes, Multi-Focus, Dynamic Distance Control of Focal Lengths and Energy Intensities at Foci.....	27
Preparation of PAN/PMMA-Based Antibacterial Carbon Nanofiber by Electrospinning Method.....	31
Preparation of Eu/Dy-doped ZnO Thin Films by Sol-Gel Process.....	37
Fully 3D Printed Bead-Pull Measurement of an Elliptical Cavity.....	42
Femtosecond Laser-Induced Filamentation Control in Liquids.....	50
Design of an Ultra-Sensitive Optical Sensor for Atmospheric Level Methane Measurement.....	54
Developing Miniaturized Orthogonal Fluxgate Sensors.....	59
Piezoelectric Based Acoustics Frequency Converter.....	67
Investigations for Increasing the Accuracy of Dielectric Constant Measurements.....	74
The Study on Noise Reduction Analysis of Untreated Leaves of Plants in Urban Areas.....	82
02. Astrophysics and Cosmology	87
Analysis of Some Semi-Detached Systems Observed by TESS.....	88
Could the CF Tuc Contain the Black Hole Closest to The Earth?.....	92

Analysis of Apsidal Motion in Eclipsing Binaries: V919 Cep and V957 Cep.....	98
Light Curve Analysis of Very Short-Period Binary System KIC 11494583.....	102
String Cloud Solutions in $f(\mathbf{R}, \mathbf{T})$ Gravity.....	106
T100 Observation of Selected Magnetic Cataclysmic Variables.....	114
Orbital Period Change of UU Leo.....	119
Searches for Uniform Metal Distributions in Galaxy Clusters.....	123
The Short-Period Eclipsing Binary 1SWASPJ173327.97+265547.9: Photometric Solution and Period Investigation.....	127
Eclipse Timing Study of a Quadruple System: KIC 7177553.....	134
A Study for KIC 5621294 and Its Component.....	139
Light Curve and Period Analysis of The Beta Lyrae Type System V359 Cas.....	145
New Transit Observation for HAT-P-36 b and HAT-P-37 b.....	152
The First Orbital Solutions of Two Eccentric Eclipsing Binary Stars From Southern: V881 Sco and GV Nor.....	157
A Comparison of the Supernovae Ratios Between the Nearby and Distant Galaxy Clusters.....	161
03. Atomic and Molecular Physics.....	167
Circular Polarization Effect Dependence of High Harmonic Generation by Excited Argon Atom.....	168
Investigation of Structural, Geometric and Radical Properties of N-Propyl Alcohol by DFT Calculations.....	173
Molecular Structure and Conformational Analysis of “Phenacetin”.....	178
Molecular Structure and Conformational Analysis of “(R)-2-Methylamino-1- Phenylethanol”.....	184
Theoretical Calculations of Electron Paramagnetic Resonance Parameters of Liquid Phase Isopropyl Alcohol.....	188
In Silico Analysis of Hair Growth Peptide.....	193
DNA Interaction of Some Hydantoin-Based Drugs with Molecular Docking Calculation.....	203

Isotope Effect on Molecular Dissociation by Intense Laser Fields in The Vicinity of Metallic Nanotip.....	210
Controlling Electron Localization in the Dissociation of H_2^+ and HD^+	217
Theoretical Calculations of Electron Paramagnetic Resonance Parameters of Acetamide in Water.....	221
A DFT Study on Molecular Structure and EPR Parameters of N, N-Dimethylformamide in Acetone and Water.....	225
Structural, Vibrational and Quantum Chemical Studies on C_{2N} (N: 0, 4, 6 and 8) Fullerenes.....	230
Quantum Chemical Investigations on C_{30} , C_{32} , C_{34} , C_{36} and C_{38} Fullerenes.....	235
Structural Correlations in Partly Quenched Two and Three Component Ionic Systems and Detecting the Structural Holes.....	241
The Life Times of Hydrogen Like Neptunium.....	244
04. Condensed Matter Physics.....	250
Characterization of Electrical Properties of PMMA/PbO Structures.....	251
Analyses of Diode Parameters Using C–V Characteristics of Al/PMMA/PbO/P-Si Structures.....	255
Janus Monolayers of MXenes: A DFT Study.....	261
Smectic Phase Transition of Ferroelectric Liquid Crystals under Influence Electric Field.....	266
The Optical and Morphological Properties of Gd doped CuO Film Using Spin Coating Method.....	274
The Structural and Electrical Properties of Cu ₂ O/ZnO Nanostructure Growth on n-type Porous Si.....	280
Investigation of Some Physical Properties of Tungsten Trioxide Thin Films Deposited via Thermionic Vacuum Arc Technique.....	285
Electrical and Morphological Properties of CuO:In Thin Films.....	293
Characterization of DLC Thin Films Deposited on Glass and Si Substrates under The Influence of Electric Field with ECR-MP Method.....	298
Enhancing Tribological Characteristics of Piston Rings of Internal Combustion Engines Using ECR-CVD Coating Method.....	304

Graphene Oxide Assembled Au-based Nanocomposite for Temperature Dependent InP Heterojunction Devices.....	307
Preparation and Characterization of Fe Doping CoO Thin Films.....	317
Optical and Morphological Studies of CoO:Ni Thin Films Grown by Ultrasonic Spray Pyrolysis.....	322
Experimental Investigation of Some Thermal Properties of Al-1,9Sc Alloy.....	327
Experimental Investigation of Some Thermal Properties of Al-6Mg-1,9Sc Alloy.....	332
The Theoretical Investigation of Antiperovskite $ANTi_3$ (A=Al, In, Tl) Compounds with DFT Calculations.....	337
Anisotropic, Elastic and Lattice Dynamical Properties of Mo_2AB (A=Al, P, Si) MAX Phase Compounds.....	345
05. Energy.....	354
Comparative Performance Analysis of Two-Bed Adsorption Cooling System Using Water Vapor Adsorption on Different Types of Silica Gel.....	355
06. High Energy and Plasma Physics.....	364
Demirci-Pro: A Single Software Interface for RFQ, Ion Source and LEBT Line Design.....	365
Investigating Magnetic Properties of YIG Thin Film Grown on Si Substrates.....	369
Investigating Magnetic Properties of NiFe Dot/Antidot Structure.....	372
Associated Production of Higgs Boson at an Electron-Photon Collision in The Two Higgs Doublet Model.....	376
Neutral Higgs Boson Pair Production via Photon-Photon Collision in The Two Higgs Doublet Model.....	381
Searching for the Dark Photon with the PADME Experiment.....	387
Review of The Nucleon to Delta Transition Axial Form Factors.....	395
07. Mathematical Physics.....	399
LRS Bianchi-Type I Space-Time in $\kappa(R,T)$ Gravity.....	400

Bianchi-Type I Universe With Dust Matter in $\kappa(R,T)$ Gravity.....	406
Cosmological Evolution and Constraint Equations in $f(G,T)$ Gravity Theory.....	411
Power-Law Solution in $f(G,T)$ Gravity.....	420
Bianchi Type-V Cosmology with Gamma Law EoS in $F(R,T)$ Gravity.....	427
The Purity and Entropy of a Multi-Site Dissipative System Driven by Random Telegraph Noise.....	432
String Cloud with Perfect Fluid Matter Distribution for Homogenous and Anisotropic Space-Time in $f(R, T)$ Gravity.....	437
Space-Time Geometry of Perfect Fluid Distribution in $f(R, T)$ Gravitation Theory.....	447
Bianchi V Universe Model for String Cloud with Perfect Fluid in Lyra Manifold.....	456
Solutions for Some DarkEnergyModels inKaluza-Klein Space-Time.....	463
Examination of Bianchi Type -VI0- for Dark Energy in $F(R,T)=R+\Lambda t$ Gravity.....	469
08. Medical Physics.....	474
CSDA Range Calculation of Proton Beam and Water Equivalent Ratio (WER) Value of Lucite ($C_5O_2H_8$).....	475
09. Nuclear Physics.....	481
A Study on TL Properties of Natural Dolomite Mineral Irradiated with Beta Particles.....	482
Nucleon Densities of Chrome Isotopes Calculation by Skyrme Interactions.....	491
Calculation of The Photomultiplier Output Voltage by FLUKA Monte Carlo Program.....	497
Energy Resolution Improvement Using Timing Method.....	503
Radiogenic Heat Productions Caused by Volcanic Tuffs Collected from Quarries in Turkey.....	511
The Excess Lifetime Cancer Risk Caused by Ingestion of Some Bottled Waters Consumed in Turkey.....	515
Electric Dipole (E1) Strength in ^{139}La Nucleus below The Neutron-Separation Energy.....	519

Radon Exhalation Rate and Effective Radium Content of the Soil Samples Collected from Orhaneli District of Bursa,Turkey	524
The Investigation of the Giant Dipole Resonance (GDR) Characteristics for ^{141}Pr Nucleus*	532
10. Statistical Physics.....	539
Phase Diagrams of Generalized Spin-S Magnetic Binary Alloys.....	540
11. Condensed Matter Physics II.....	547
Zinc Molar Concentration Induced Structural and Optical Properties of Chemically Derived ZnS Thin Films.....	548

09. Nuclear Physics



Türk Fizik Derneği
— 1950 —
Turkish Physical Society

A Study on TL Properties of Natural Dolomite Mineral Irradiated with Beta Particles

S. Akça^{1, a)}

¹*Çukurova University, Faculty of Arts and Sciences, Department of Physics, Adana, Turkey*

^{a)}*Corresponding author: sblakca@gmail.com*

Abstract. The present study aims to reveal thermoluminescence (TL) features of natural dolomite mineral. In the first stage, the proper filter was selected as WBB with HR of $2\text{ }^{\circ}\text{Cs}^{-1}$ from RT to $450\text{ }^{\circ}\text{C}$. The results obtained from TL glow curves showed that the curves were composed of two peak maxima (pm) located at 102 and $252\text{ }^{\circ}\text{C}$ at doses between 0.11 - 10 Gy . When examined the dose dependence of each peak maxima, each of them exhibited a good linear response. The mineral was found to be reusable within 8% and 16% for peak 1 and 2, respectively. The effects of the HRs in the range of 0.5 - $10\text{ }^{\circ}\text{Cs}^{-1}$ on TL were researched taking into account the change of the FWHM, T_m , I_m and peak area vs HR for each pm and observed an anomalous case increasing TL intensity with HR. The T_m - T_{stop} experiment and CGCD analyses performed showed that the curves consist of at least 8 superposition peaks. The E_a values are in good agreement at both methods and found to be 0.65 - 1.08 (p1) and 1.4 - 1.71 eV (p2) applying CGCD method.

INTRODUCTION

Dolomite ($\text{CaMg}(\text{CO}_3)_2$) is a common mineral consisting of alternate layers of calcite CaCO_3 and magnesite MgCO_3 used mostly in industrial fields. One of the most important application areas of dolomite mineral is to use in the production of fire-resistant materials, used in metallurgy, chemical and ceramic industries [1–2]. In recent years, besides, several studies on thermoluminescence (TL) characteristic of this mineral have been performed by the irradiation with gamma rays in general [3-6].

In a study on TL of natural dolomite, Soliman et al. observed that the glow curve of the blue emission band in TL in the range from room temperature (RT) to $400\text{ }^{\circ}\text{C}$ had peaks at 240 and $270\text{ }^{\circ}\text{C}$ with a heating rate (HR) $4\text{ }^{\circ}\text{C/s}$. The laboratory induced glow curve had 10 peaks between 145 and $355\text{ }^{\circ}\text{C}$ for a gamma dose of 10^4 Gy and the TL response to gamma-rays was found to be linear over the dose range 500 - 10^4 Gy [3]. Ramasamy et al. studied on features of TL glow curve of ten dolomitic crystals. Two peaks at $270\text{ }^{\circ}\text{C}$ and $335\text{ }^{\circ}\text{C}$ were observed in the natural thermoluminescence (NTL) measurements whereas an extra peak at $180\text{ }^{\circ}\text{C}$ appeared when the sample had been exposed to a gamma dose of 200 Gy . Annealing experiments of the samples were carried out at the temperatures in the range of 200 - $950\text{ }^{\circ}\text{C}$ for all three TL peaks and annealing temperature of $700\text{ }^{\circ}\text{C}$ for 4 h followed by quenching in air was found to be in the optimum condition for TL. They also evaluated the kinetic parameters of dolomite crystal using peak shape (PS) and initial rise (IR) method and concluded that the trapping centers were not influenced by the annealing process [4]. A theoretical study on concentration quenching (CQ) of TL in dolomite was also performed by Mostefa el al. It was carried out using the model of 5TOR. The simulated results achieved using their model were found in harmony with the experimental results put submitted previously in the literature [5]. Soliman et al. studied again on natural dolomite and observed that their natural dolomite sample gave two peaks at $240\text{ }^{\circ}\text{C}$ and $325\text{ }^{\circ}\text{C}$ in the green region and four peaks at 225 , 240 , 270 and $325\text{ }^{\circ}\text{C}$ in the red region. They also obtained sublinearity for both bands in the range of 1 - 100 Gy and linearity in the region 200 - 10^4 Gy at the dose response curves [6].

In the present study, dose-response, reusability, heating rate (HR) effect and kinetic parameters (activation energy (E_a), frequency factor (s) and order of kinetic (b)) of natural dolomite samples were investigated to determine the TL properties of the mineral. To evaluate the kinetic parameters, T_m - T_{stop} experiment and CGCD (Computed Glow Curve Deconvolution) analyses were carried out.

MATERIAL AND METHODS

The natural dolomite samples were supplied from Mersin province in Turkey. The samples were ground to a powder with an agate mortar, and the powdered samples were sieved at the size of 90 μm then placed in Eppendorf tubes. The powder samples of 25 mg pressed with pressure of 2 tons/cm² during 20 minutes were converted to thin pellet form before being analyzed and measured.

All TL measurements of the pellets were performed using an automated Lexsyg Smart TL/OSL reader system having different filter combinations. The reader system has an internal ⁹⁰Sr/⁹⁰Y source with 1.95 GBq emitting beta particles with a maximum energy of 2.2 MeV and a dose rate of 0.11 Gys⁻¹.

The pellet samples of 25 mg were heated from RT to 450 °C to eliminate the previous history of any geological information prior to irradiation. In the first stage of the experiment, TL glow curves of the filter test performed using different band filters were recorded with a constant HR of 2 °Cs⁻¹ from RT to 450 °C after a dose of 5 Gy. The TL glow curves to observe dose-response were also recorded at the dose in the range of 0.11–10 Gy with beta irradiation. In addition, the TL curves of the HRs in the range of 0.5–10 °Cs⁻¹ and reusability test were performed with beta dose of 5 Gy.

RESULTS AND DISCUSSION

Optimum Filter

The selection of the best suitable filter is of great importance to observe the TL signal more efficiently. The automated Lexsyg Smart TL/OSL reader used in this study provides the opportunity to choose the desired one among various types of band pass filters inserted between the sample and the photomultiplier tube (PMT). The pellet samples were exposed to a constant beta dose of 5 Gy for suitable filter selection. Fig. 1 displays a comparison of IRSL wideband blue (WBB), BSL 365 nm, IRSL 410 nm, and IRSL 565 filters. It can be easily seen from Fig. 1, the highest TL intensity has been obtained using WBB filter and there are two peak maxima centered at 102 and 252 °C. In the lights of these results, TL measurements in the present study were carried out using the WBB filter.

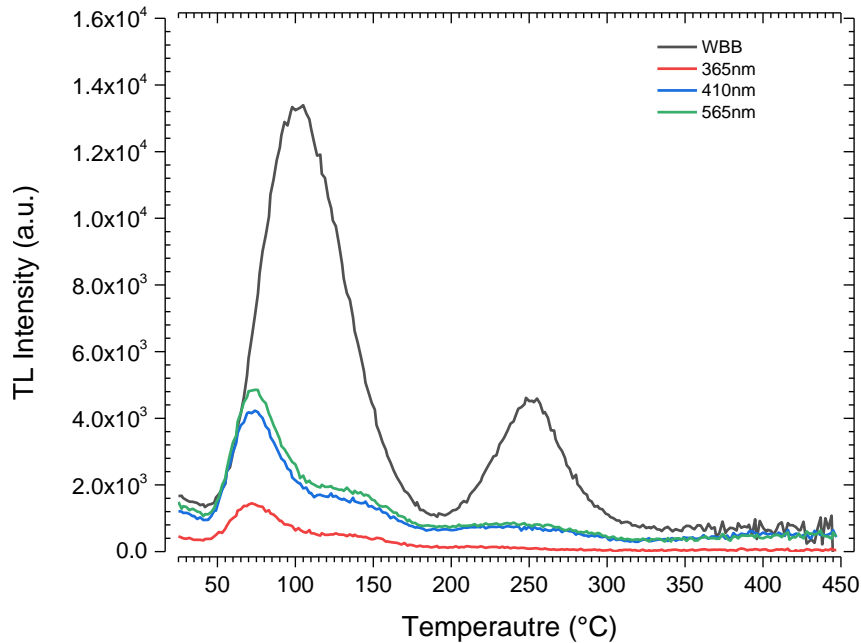


FIGURE 1. The results of filter test of natural dolomite mineral at dose of 5 Gy with heating rate of 2 °Cs⁻¹

Dose-Response

A good TL material is expected to respond to different dose levels with the same precision. To evaluate dose-response of the dolomite pellets TL glow curves were recorded at low beta doses in the range of 0.11 – 10 Gy. Fig. 2 shows TL glow curves of the pellets at the dose of 0.11, 1, 3, 5, 8 and 10 Gy. As seen in Fig. 2, the curves compose of two peak maxima up to 10 Gy and the TL intensity increased with the increasing beta doses.

In addition, to see the relation between TL intensity and irradiation dose more clearly, a figure (Fig. 3) that shows the change of peak area versus beta dose is plotted using an equation of the form; $TL = aD^b$. When examined the dose dependence of each peak maxima, according to area under each peak maxima, each of them exhibits a good linear response with linearity parameters of $b=1.03$ and $b=1.17$ for peak-1 and peak 2, respectively.

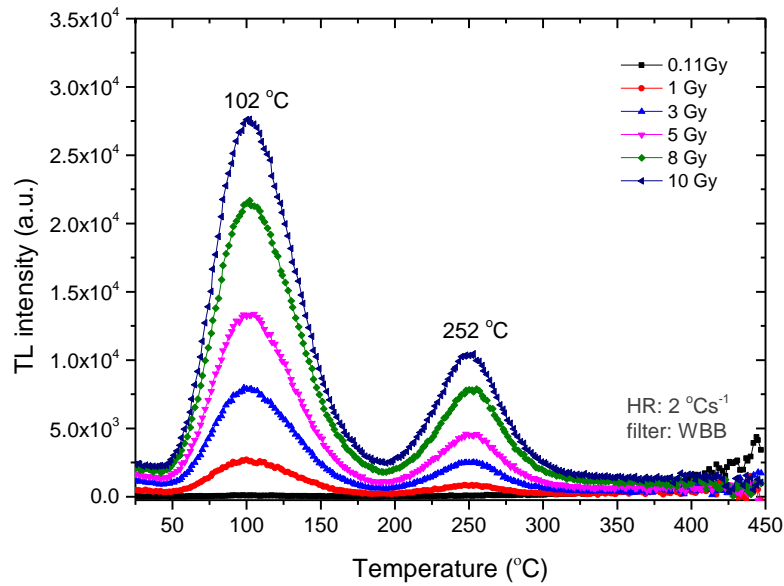


FIGURE 2. TL responses versus doses between 0.11-10 Gy of natural dolomite mineral

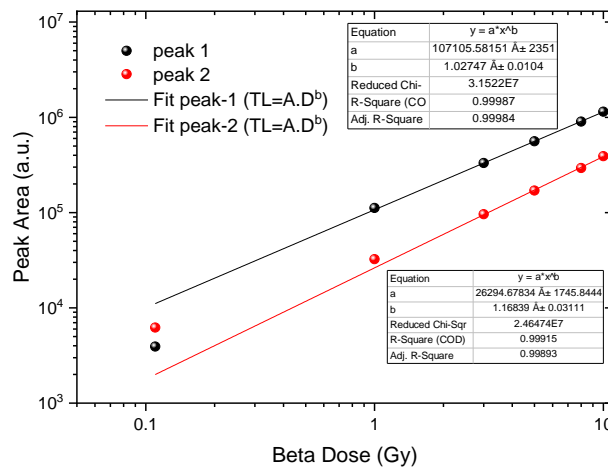


FIGURE 3. The change of peak area versus the dose of natural dolomite mineral for peak 1 and peak 2

Heating Rate

TL peak shape and position show changes depending on the heating rate (HR). Thus, the influences of the HRs in the range of $0.5\text{--}10\text{ }^{\circ}\text{Cs}^{-1}$ on TL glow peak of natural dolomite pellet were examined with beta irradiation of 5 Gy. The effects of the HRs are presented in Fig.4. One can see in Fig.4 that (the unit of TL intensity is given as $\text{count}/^{\circ}\text{C}$) the peak maxima temperatures of the glow curve shift to higher temperatures with increasing HR. Besides, it is seen in the figure that behavior of TL intensity of the glow peaks does not exhibit the expected result in the TL theory [7]. The intensity of TL glow peak maxima increases with an increase at HR, which is known as anomalous heating rate effect. Such an anomalous effect can be resulted from an increase in the probability of radiative transitions compared to that of the non-radiative transitions [8].

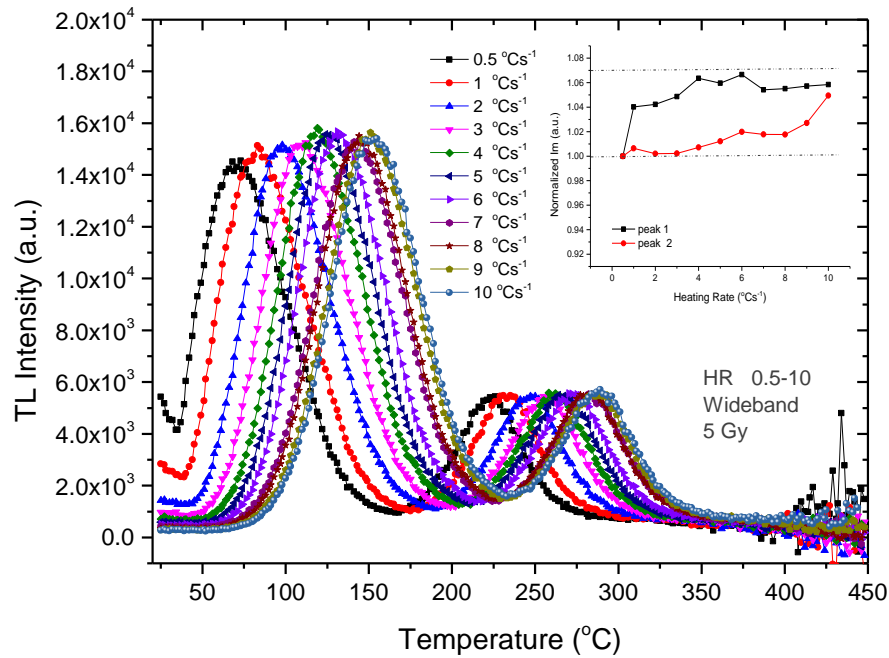


FIGURE 4. TL glow curves of natural dolomite mineral measured at various heating rates from 0.5 to $10\text{ }^{\circ}\text{Cs}^{-1}$. Inset Figure shows the normalized maximum intensity (I_m) versus heating rate for peak 1 and 2.

To examine the influence of HR in detail, the graphs of the change of the normalized peak area, peak maxima temperature (T_m) and the full width at the half maximum (FWHM) versus HR for each peak maxima were plotted (Fig. 5 (a), (b), (c)). The area under the TL peak maxima increases in the rate of about 15% by the increase of HR for peak 1 and 2 (Fig. 5(a)). The T_m shifts to the higher temperatures with increasing HR (Fig. 5(b)). Besides, when examined the behavior of the FWHM of natural dolomite pellets versus HR (Fig. 5(c)), it is observed that the glow peak comparatively becomes much wider for both peak maxima.

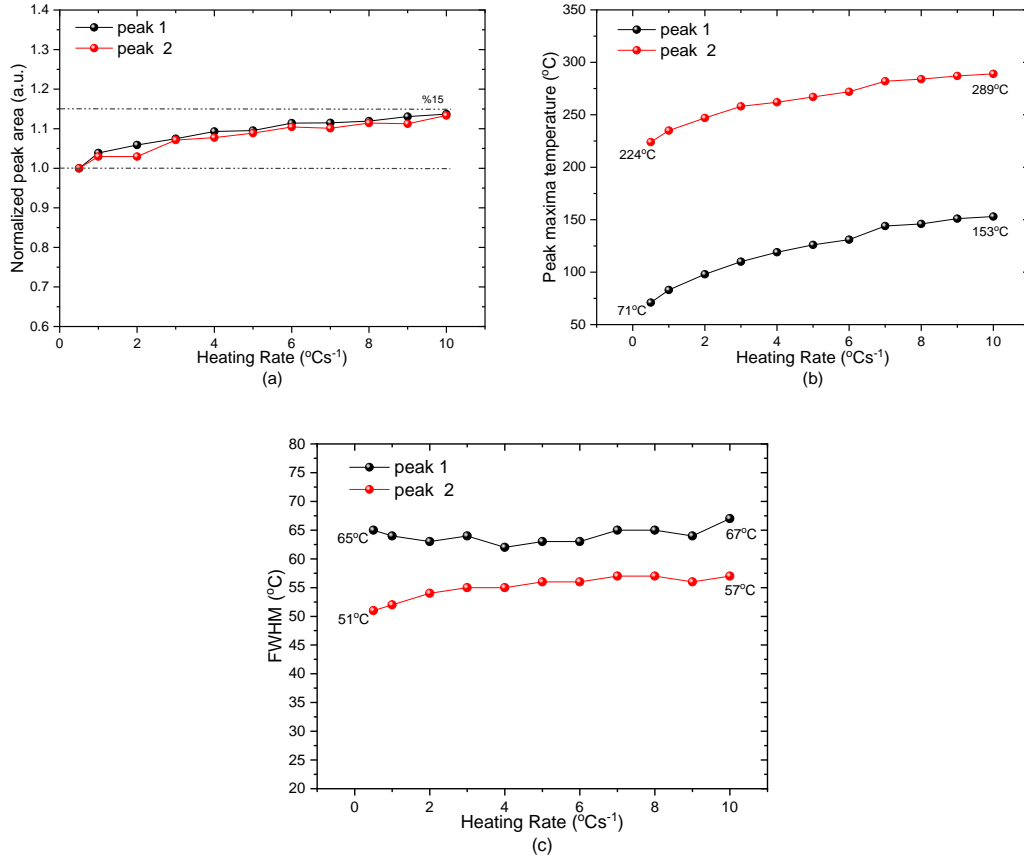


FIGURE 5. The change of (a) the normalized peak area (b) the peak maxima temperature (c) FWHM versus heating rate for peak 1 and peak 2 of natural dolomite mineral

Reusability

The reusability test determines if TL signal from material exhibits any changes when exposed to the same conditions. In this experiment, the readouts of the glow curve were carried out for 9 sequential measurements with dose of 5 Gy at a linear HR of 2 °Cs⁻¹ and the results revealed that the mineral is reusable within 8% and 16% for peak 1 and 2, respectively (Fig. 6). Actually, reusability of a good TL material should have less than 5% for sequential measurements under the same dose and readout conditions [9]. However, natural materials can give higher value than 5% at reusability test due to impurities in natural mineral or new traps that occur depending on the radiation exposure at each cycle [10-12].

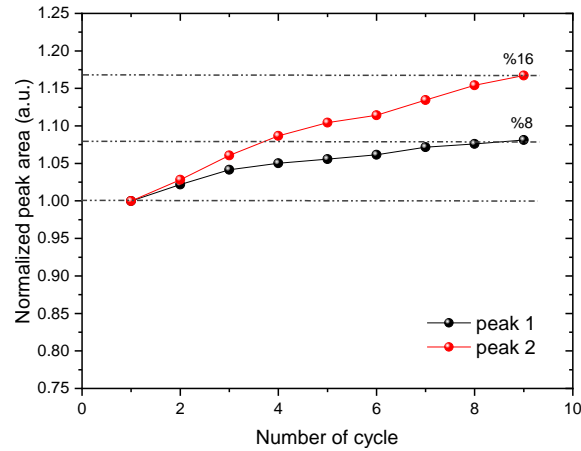


FIGURE 6. The behavior of normalized peak area for peak 1 and peak 2 through 9 consecutive cycles of natural dolomite mineral

The Evaluation of Kinetic Parameters

$T_m - T_{stop}$ experiment

$T_m - T_{stop}$ experiment has been performed in the literature to decompose TL glow curves consisting of overlapping peaks [13]. In this study, $T_m - T_{stop}$ experiment was carried out to deconvolve the overlapping peaks and determine the order of kinetics (b), activation energy (E_a) and frequency factor (s). The natural dolomite pellet irradiated with a beta dose of 5 Gy was heated up to a T_{stop} at HR of 2 °Cs⁻¹ and cooled to RT. Then TL readouts were performed up to 450 °C. The sample irradiated with the same dose was reheated to a new T_{stop} with the increment of 5 °C and the cycles were repeated in the complete interval $T_{stop} = 45-320$ °C. Thus, clean peaks for each curve were obtained in order to apply the initial rise (IR) method after $T_m - T_{stop}$ experiment and the activation energies and frequency factors given in Table 1 were estimated for probable deconvolved peaks. In addition, a plot of the calculated activation energy (E_a) versus T_{stop} is shown as Fig. 7. The figure indicates that the main peaks consist of at least eight superposition peaks.

TABLE 1 The values of activation energy E (eV) and frequency factor s (s⁻¹) obtained using the initial rise (IR) method after $T_m - T_{stop}$ experiment.

The obtained peaks	T_{stop} range (°C)	E (eV)	s (s ⁻¹)
1 st Peak	45-90	0.55-0.64	8.2E+07-1.4E+08
2 nd Peak	95-135	0.78-0.80	3.6E+08-1.4E+10
3 rd Peak	140-165	0.81-0.83	7.4E+07-5.6E+08
4 th Peak	170-185	1.13-1.16	1.7E+11-4.1E+11
5 th Peak	190-215	1.42-1.44	8.7E+13-1.3E+14
6 th Peak	220-250	1.54-1.56	9.9E+13-1.2E+15
7 th Peak	255-285	1.63-1.66	1.4E+13-5.4E+14
8 th Peak	290-320	1.70-1.84	6.3E+12-3.9E+14

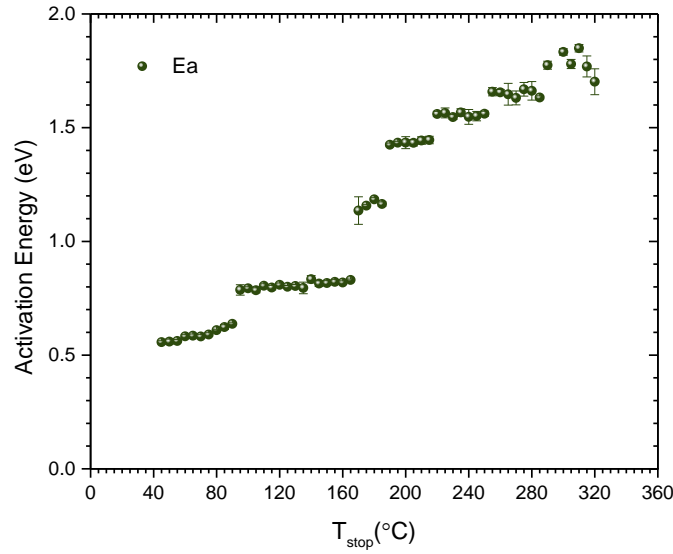


FIGURE 7. The change of the activation energy versus T_{stop} obtained after T_m - T_{stop} experiment with dose of 5 Gy at HR of 2 °Cs⁻¹ of natural dolomite mineral.

CGCD Method

CGCD (Computerized Glow Curve Deconvolution Method) is a useful method for analysis of the main peaks that includes overlapping TL glow peaks. This method also allows to evaluate the kinetic parameters without the need of any further thermal annealing. The experimentally obtained glow curve with the readouts at a HR of 2 °Cs⁻¹ after beta irradiation under 5 Gy dose was deconvolved applying general order kinetic equation which Chen, and Kitis et al. [14-16] have contributed using R-software package “tgcd” [17]. Fig. 8 shows the deconvolution results consisting of at least eight superposition peaks of natural dolomite pellet. Figure of merit (FOM) value which is a sign of agreement between experimental and theoretical data was found to be 1.67%. The FOM value should be less than 5% considering acceptable fit value.

The best estimates of kinetic parameters of the deconvolved peaks are given in Table 2. As seen in Table 2, the activation energy values were found to be 0.65-1.08 (Peak 1 maxima) and 1.4-1.71 eV (Peak 2 maxima). The orders of kinetic were determined to be in the range of 1.44-2. In addition, s values were found to be in the range of 10⁸-10¹⁴, as expected.

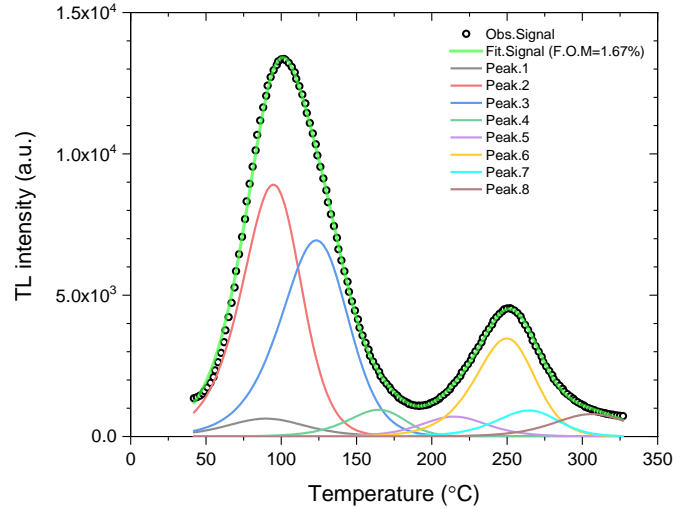


FIGURE 8. Deconvolution of the glow curve at 5 Gy dose of natural dolomite mineral.

TABLE 2 The values of maximum peak temperature $T_m(^{\circ}\text{C})$, the activation energy E (eV), frequency factor s (s^{-1}) and kinetic order b of deconvolved peaks obtained by the deconvolution of the main peak of natural dolomite sample using CGCD method (HR: 2°C s^{-1} , irradiation dose: 5 Gy)

Deconvolved Peaks	$T_m(^{\circ}\text{C})$	E (eV)	s (s^{-1})	b
1 st Peak	89.85	0.65	$1.10\text{E}+08$	2
2 nd Peak	94.77	0.79	$8.15\text{E}+09$	1.6
3 rd Peak	123.34	0.8	$1.66\text{E}+09$	1.6
4 th Peak	164.85	1.08	$3.39\text{E}+11$	1.44
5 th Peak	214.85	1.4	$3.70\text{E}+13$	2
6 th Peak	249.85	1.58	$2.18\text{E}+14$	1.6
7 th Peak	264.59	1.6	$1.23\text{E}+14$	1.6
8 th Peak	306.37	1.71	$8.30\text{E}+13$	2

CONCLUSION

In the present study, dose-response, reusability, heating rate (HR) effect and kinetic parameters of natural dolomite mineral supplied from Mersin province were examined in order to determine the TL properties of the samples. The results of the measurements revealed that TL response at low beta doses between 0.11 and 10 Gy exhibited good linearity. Heating rate effect on TL signal showed an anomalous state that TL intensity enhances with increasing HR due to an increase in the probability of radiative transitions compared to that of the non-radiative transitions. The reproducibility results of the natural dolomite samples were examined and the obtained results were found to be in the acceptable limits when compared with the reproducibility results of natural materials. To find the kinetic parameters of TL glow curves of the mineral, $T_m - T_{stop}$ and CGCD Methods were used, and the results obtained using these methods were found to be in good agreement.

These experiments and calculations performed up to now is a preliminary study to learn TL properties of dolomite mineral. For future studies, dolomite mineral samples will be annealed to make them more stable and the measurements and calculations will be performed again for the annealed samples to compare both results and to learn whether the mineral can be used as a dosimetric material.

ACKNOWLEDGMENTS

This work was supported by the Research Fund of the Çukurova University, Turkey (Project Number: FBA-2018-10828).

REFERENCES

1. G.S. Gai, Y.F. Yang, S.M. Fan, Z.F. Cai, Powder Technol. **153**, 153–158 (2005).
2. M. Rabah, E.M.M. Ewais, Ceram. Int. **35**, 813–819 (2009).
3. C. Soliman , A.M. Massoud, M.A. Hussein, Nucl. Instrum. Meth. B **222**, 163–168 (2004).
4. V. Ramasamy, V. Ponnusamy, S.S. Gomathi, M.T. Jose. Radiat. Meas. **44**, 351–358 (2009).
5. R. Mostefa, A. Kadari, S. Hiadsi, D. Kadria. Optik **127**, 368–370 (2016).
6. C. Soliman, S.M. Metwally, F.F. Alharbi, K.M. Elshokrofy. Journal of Taibah University for Science **11**, 534–539 (2017).
7. J.T. Randall, M.H.F. Wilkins, and M.L.E, Proc. R. Soc. Lond. A **184**, 366-389 (1945).
8. S. Delice, E. Bulur, and N.M. Gasanly, J. Mat. Sci. **49**, 8294-8300 (2014).
9. Furetta C. Handbook of thermoluminescence, World Scientific, Singapore, 2003.
10. H. Tugay, Z. Yegingil, T. Dogan, N. Nur, N. Yazici, Nucl. Instr. Meth. Phys. Res. B **267**, 3640–3651(2009).
11. M. Sardar, M. Tufail, Nucl. Instr. Meth. Phys. Res. B **269**, 284–287 (2011).
12. N. Nur, Z. Yegingil, M. Topaksu, K. Kurt, T. Dogan, N. Sarigül, M. Yüksel, V. Altunal, A. Özdemir, V. Güçkan, I. Günay. Nucl. Instr. Meth. Phys. Res. B **358**, 6–15 (2015).
13. K.H. Nicholas and J. Woods, British Journal of Applied Physics. **15**, 783–795 (1964).
14. R. Chen, J. Electrochem. Soc. **116** (9), 1254–1257 (1969a).
15. R. Chen, J. Appl. Phys. **40**, 570–585 (1969b).
16. G. Kitis, J.M. Gomez-Ros, J.W.N. Tuyn, J. Phys. D. Appl. Phys. **31**, 2636–2641 (1998).
17. J. Peng, Z. Donga and F. Han, SoftwareX **5**, 112–120 (2016).